ChemComm

Dynamic Article Links ►

Cite this: DOI: 10.1039/c0xx00000x

www.rsc.org/xxxxxx

COMMUNICATION

Direct synthesis of novel homogeneous nanocomposites of Li_2MnSiO_4 and carbon as a potential Li-ion battery cathode material

Shintaro Aono,[a] Taisuke Tsurudo,[b] Koki Urita[b] and Isamu Moriguchi*[b]

Received (in XXX, XXX) Xth XXXXXXXXX 20XX, Accepted Xth XXXXXXXXX 20XX

DOI: 10.1039/b000000x

Homogeneous nanocomposites of nanocrystalline Li_2MnSiO_4 and carbon as well as a carbon nanotubes-embedded nanocomposite are synthesized directly by a novel method using organic-inorganic hybrid polymers which consist of covalently bonded phenolic oligomer and siloxane parts. The nanocomposites show superior charge-discharge performance at room temperature in spite of low carbon contents.

There has been intensive interest in the development of electrode materials for lithium ion secondary batteries with both high energy and high power densities due to expected demand for power-grid applications as well as power sources of electric and hybrid electric vehicles. Polyanion-based cathode materials such as $LiMPO_4$ and Li_2MSiO_4 (M = Fe, Mn) have been widely investigated as candidates for cathode materials because of their practical merits of safety, low cost and environmental benignity.[1,2] Since these materials have inherently poor electronic conductivity and Li-ion diffusivity, down-sizing of active materials and conductive phase embedding have been actively studied to overcome the latent problem,[3–17] which lead actually the successful development of $LiFePO_4$ as an alternative to conventional metal oxide-base cathode materials. In recent years, orthosilicates, Li_2MSiO_4 (M = Fe, Mn), have attracted growing interest as highly capacitive cathode materials, of which specific capacities are considered to exceed 330 mAh g^{-1} theoretically if 2 Li ions per formula unit contribute to charging and discharging reactions. However, low capacities corresponding to the extraction/insertion of less than 1 Li ion per formula unit (i.e., < 160 mAh g^{-1}) were realized in practice for most of the studies on the development of orthosilicate cathodes.[12–17] The major drawback of orthosilicates is their very low intrinsic conductivities; especially, the conductivity of Li_2MnSiO_4 is below 10^{-16} S cm^{-1} at room temperature,[18] which is about five orders of magnitude lower than that of $LiMnPO_4$.[19]

Very recently, some reports have achieved high initial capacities over 200 mAh g^{-1} for Li_2MnSiO_4 nanocrystallites post-coated with conductive materials,[20–23] indicating the possibility of extraction of more than 1 Li ion from Li_2MnSiO_4. However it is worth noting that such high capacity was obtained in the presence of much amount of conductive materials in the electrode and the capacity faded in the early stage of charge-discharge cycles.[20–23] In addition, some of the reported Li_2MnSiO_4 cathodes showed lowering the average discharge potential, which means the decrease in energy density.[21–23] To enhance the electrode performance, the composite structure of Li_2MnSiO_4 and a conductive material should be precisely controlled in nanoscale for effective Li ion and electron transports with the minimized amount of conductive materials. In this context, so far reported methods such as post carbon-coating of active material nanoparticles do not always meet the requirements due to the strong agglomeration of nanoparticles which prevents homogeneous mixing with a conductive material.

Herein we propose a novel method to synthesize homogeneous nanocomposites of nanocrystalline Li_2MnSiO_4 and carbon by using organic-inorganic hybrid polymers with the chemical structure indicated in Fig. 1, where phenolic oligomer and siloxane parts can be converted into carbon and silicate via a calcination, respectively. The new attempt using such hybrid polymers as both carbon and mineral sources has advantages of production of carbon nanophases nearby active material nanocrystals and suppression of the crystal growth to yield homogeneous conductive nanocomposites directly. The present study have succeeded in the synthesis of homogeneous nanocomposites of nanocrystalline Li_2MnSiO_4 and carbon as well as embedding carbon nanotubes (CNTs) in them to form hierarchical conducting paths. It was also demonstrated that the hybrid polymer-derived nanocomposites show superior charge-discharge properties with a reasonable discharge potential and appropriate carbon content, and the introduction of small amount of CNTs enhances the properties.

Nanocomposites of Li_2MnSiO_4 and carbon were synthesized by a sol-gel process using commercial organic-inorganic hybrid polymers (Arakawa Chemical Industries, Ltd.), COMPOCERAN P501 and HBP70, which have the composition of 40 wt% and 70 wt% SiO_2 in their hardening resins, respectively. Mn and Li sources were mixed with the polymer in ethanol with the stoichiometric molar ratio (Li/Mn/Si=2/1/1), and the obtained gel was subjected to pre-

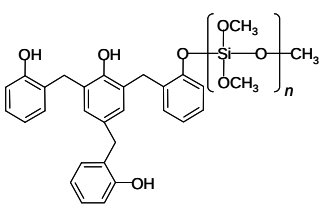

Fig. 1 Chemical structure of the organic-inorganic hybrid polymer

Table 1 Structural characteristics of the samples

Sample	d (nm)[a]	C-content (wt%)[b]	Sa ($m^2 g^{-1}$)[c]
Bulk-LMS	26	2.4	19
LMS-P501	8	27.0	203
LMS-HBP70	19	9.8	108
LMS-HBP70-CNT	21	14.5	108

[a] Primary crystallite size of Li_2MnSiO_4 determined from FWHM of (010) XRD peak. [b] Carbon content estimated by elementary analysis. [c] Specific surface area determined by Brunauer-Emmett-Teller (BET) method from N_2 adsorption isotherms.

calcination at 500 °C, ball-milling and the calcination at 650 °C in order (see experimental details in ESI†). Hereafter, the composite samples obtained by using COMPOCERAN P501 and HBP70 are abbreviated as LMS-P501 and LMS-HBP70, respectively. A nanocomposite of LMS-HBP70 and CNTs, which is denoted as LMS-HBP70-CNT, was also synthesized by the similar synthetic procedure of LMS-HBP70 using a CNTs-dispersed ethanol solution instead of the ethanol mentioned above. As a reference, a Li_2MnSiO_4 sample without CNTs, Bulk-LMS, was synthesized by using $Si(CH_3COO)_4$ instead of the hybrid polymer.

The composition of Li, Mn and Si in obtained samples was confirmed by elemental analysis to be close to the stoichiometry of Li_2MnSiO_4 although a small excess amount of Si existed (Table S1, ESI†). All the X-ray diffraction (XRD) peaks of samples were in good agreement with the orthorhombic crystal structure ($Pmn2_1$) of Li_2MnSiO_4 (Fig. S1, ESI†). Primary crystallite size, carbon contents and BET surface areas of samples were listed in Table 1. The samples obtained by using the hybrid polymers had obviously higher carbon contents than bulk-LMS. The residual carbons in LMS-P501 and LMS-HBP70 were originated from the phenolic oligomer moieties in the hybrid polymers, of which carbonization ratio was 66−68 wt% at 650 °C for both polymers. The difference in carbon content between LMS-HBP70 and LMS-HBP70-CNT was almost consistent with the weight ratio of CNTs introduced in the synthesis. It was observed by transmission electron microscopy (TEM) that LMS-P501 and LMS-HBP70 were composed of Li_2MnSiO_4 nanocrystallites and residual amorphous carbons (Fig. 2a and b). The carbons were deposited on the surface and the interstitial space of Li_2MnSiO_4 single-crystalline nanoparticles (Fig. 2c). As shown in Fig. 2d and 2e, the size of nanoparticles is almost uniform around 8 and 19 nm for LMS-P501 and LMS-HBP70, respectively, which are in good agreement with the primary crystallite size estimated from the full width at half-maximum (FWHM) of the XRD peak of (010) plane using the Scherrer equation (Table 1). The homogeneous nanocomposite structure of hybrid polymer-derived samples resulted in their high specific surface areas in contrast to the quite low specific surface area of bulk-LMS having the primary crystallite size of 26 nm. This suggests that Li_2MnSiO_4 nanocrystallites with the uniform size are highly dispersed in the nanocomposites to provide accessible large interface which is desirable for charge transfer reactions. Formation of a nanocomposite of LMS-HBP70 and CNTs was also confirmed for LMS-HBP70-CNT as shown in Fig. 2f and Fig. 2S in ESI†, where CNTs were successfully incorporated in the composite while keeping the nanocrystallite-assembly structure of LMS-HBP70.

Electrochemical charge-discharge measurments were carried out by the constant current and subsequent constant voltage (CC-CV) mode charging and CC mode discharging at the current density of 16.6 mA g^{-1} in a 1.0 mol dm^{-3} solution of $LiPF_6$ in ethylene carbonate/dimethyl carbonate against metallic Li at room temperature (see experimental details in ESI†). The samples mixed with poly(tetrafluoroethylene) (PTFE) and additionally acetylene black (AB) were pressed on Al mesh, and then were used as working electrodes; the weight ratio of sample/AB/PTFE was 62.5/25/12.5 for Bulk-LMS, 85/10/5 for LMS-HBP70, and 90/0/10 for LMS-P501 and LMS-HBP70-CNT. Fig. 3a shows initial charge-discharge

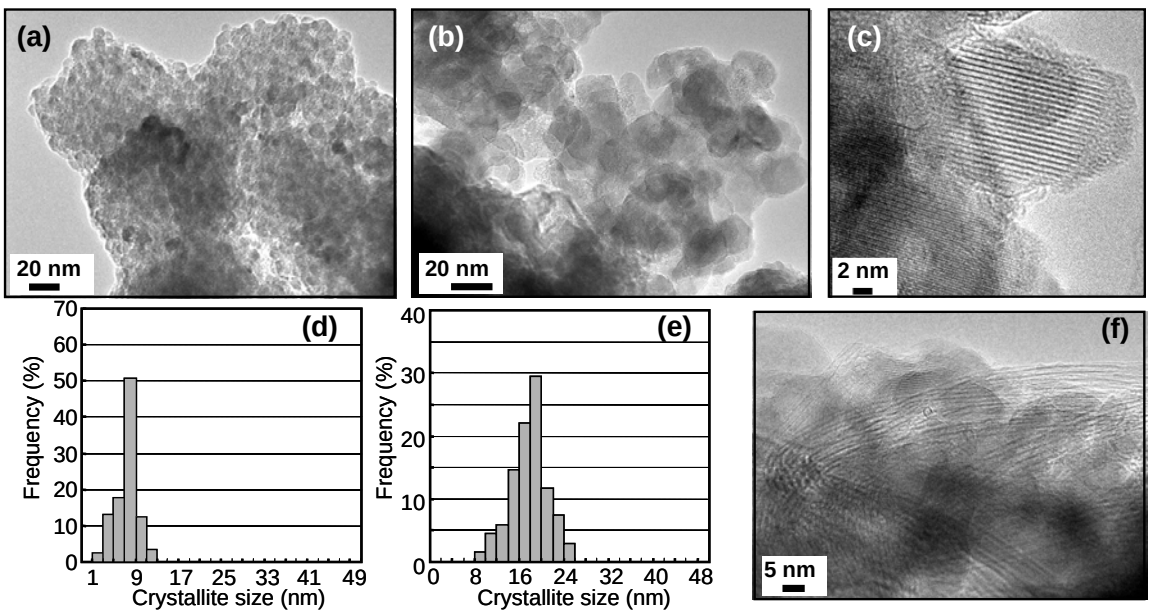

Fig. 2 TEM images of (a) LMS-P501, (b) LMS-HBP70, and (c) an enlarged part of LMS-HBP70. (d) and (e) Particle size distributions of LMS-P501 and LMS-HBP70, respectively. (f) TEM image of LMS-HBP70-CNT.

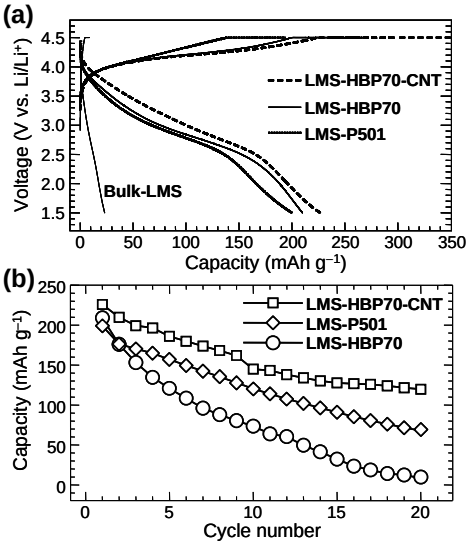

Fig. 3 (a) Initial charge-discharge curves, and (b) cycle performance of the samples.

curves of the samples at room temperature. The hybrid polymer-derived samples showed initial discharge capacities above 200 mAh g^{-1}; the capacities of LMS-P501, LMS-HBP70 and LMS-HBP70-CNT were 200, 210 and 226 mAh g^{-1}, which correspond to 1.21, 1.27 and 1.36 Li ions insertion per formula unit, respectively. High initial discharge capacities over 1 Li insertion per formula unit for Li_2MnSiO_4 nanocrystallites at room temperature were observed in some recent reports, but the amount of conductive additives in their electrodes was ca. 25−30 wt%[20,22,23] and some of their average discharge potentials were almost the same as or lower than that of Li_2FeSiO_4 so far reported (~ 2.6 V).[22,23] The present nanocomposite cathodes have lower carbon contents in electrode of 13.0−24.3 wt% and higher average discharge potential around 3.0 V. The homogeneous nanocomposite structure of Li_2MnSiO_4 nanocrystallites and carbons is effective to yield high capacities in spite of the low carbon contents. LMS-HBP70-CNT, which has the lowest carbon content in the electrode (13 wt%), shows the highest capacity among so far reported Li_2MnSiO_4 cathodes having the reasonable average discharge potential. The capacity of only CNTs in the composite was considered to be below 2 mAh g^{-1} taking into acount of the incorporated amount, which is negligibly small (Fig. S3, ESI†). Therefore, the achievement of high capacity for LMS-HBP70-CNT is ascribable to a formation of hierarchical conducting paths throughout the hybrid polymer-derived homogeneous nanocomposite by the incorporation of a small amount of CNTs. As shown in Fig. 3b, the capacities of nanocomposite samples faded gradually with charge-discharge cycles. It was reported for Li_2MnSiO_4 cathodes having such high initial capacities that the capacity retentions at room temperature became below 50% within 20 cycles.[20,22,23] On the other hand, LMS-HBP70-CNT shows higher capacity retention of 53% after 20 cycles

In conclusion, homogeneous nanocomposites of nanocrystalline Li_2MnSiO_4 and carbon as well as a CNTs-embedded nanocomposite were successfully synthesized by the novel method using organic-inorganic hybrid polymers. The production of mono-dispersed Li_2MnSiO_4 nanocrystallites and their homogeneous mixing with carbon materials in nanometer scale provide short reaction pathways for lithium insertion/extraction accompanied with effective electron conduction, which resulted in superior charge-discharge performance at room temperature. Further study is now in progress to enhance the kinetics and cycling stability of the new nanocomposites by optimizing the crystalline size, composition and so on.

The study made use of instruments (elementary analysis, XRD, and TEM) in the Center for Instruments Analysis of Nagasaki University. This work was supported by a grant for Advanced Low Carbon Technology Research and Development Program (ALCA) from Japan Science and Technology Agency (JST).

Notes and references

[a] *Graduate School of Science and Technology, Nagasaki University, 1-14 Bunkyo-machi, Nagasaki 852-8521, JAPAN, E-mail: d710201j@cc.nagasaki-u.ac.jp*
[b] *Division of Chemistry and Materials Science, Graduate School of Engineering, Nagasaki University, 1-14 Bunkyo-machi, Nagasaki 852-8521, JAPAN, E-mail: mrgch@nagasaki-u.ac.jp*

† Electronic Supplementary Information (ESI) available: [Experimental details, XRD patterns of samples]. See DOI: 10.1039/b000000x/

1 B. Kang, G. Ceder, *Nature*, 2009, **458**, 190
2 M. S. Islam, R. Dominko, C. Masquelier, A. R. Armstrong, P. G. Bruce, *J. Mater. Chem.*, 2011, **21**, 9811.
3 P. Gibot, M. C-Cabanas, L. Laffont, S. Levasseur, P. Carlach, S. Hamelet, J.-M. Tarascon, C. Masquelier, Nature Mater. 2008, 7, 741.
4 Y-.H. Huang, K-.S. Park, J. B. Goodenough, *J. Electrochem. Soc.* 2006, **153**, A2282.
5 K. Striebel, J. Shim, A. Sierra, H. Yang, X. Song, R. Kostecki, K. McCarthy, *J. Power Sources*, 2005, **146**, 33.
6 Y. Wang, J. Wang, J. Yang, Y. Nuli, *Adv. Funct. Mater.*, 2006, **16**, 2135
7 S. Aono, K. Urita, H. Yamada, I. Moriguchi, *Solid State Ionics*, 2012, **225**, 556.
8 I. Moriguchi, S. Nabeyoshi, M. Izumi, H. Yamada, *Chem. Lett.*, 2012, **41**, 1639.
9 A. R. Armstrong, N. Kuganathan, M. S. Islam, P. G. Bruce, *J. Am. Chem. Soc.*, 2011, **133**, 13031.
10 X. Wu, X. Jiang, Q. Huo, Y. Zhang, *Electrochim. Acta*, 2012, **80**, 50.
11 Y. Zhao, J. Li, C. Wu. Y. Ding, L. Guan, *J. Mater. Chem.*, 2012, **22**, 18797.
12 R. Dominko, M. Bele, M. Gaberscek, A. Meden, M. Remskar, J. Jamnik, *Electrochem. Commun.*, 2006, **8**, 217.
13 R. Dominko, *J. Power Sources*, 2008, **184**, 462.
14 H. Duncan, A. Kondamreddy, P. H. J. Mercier, Y. L. Page, Y. A-. Lebdeh, M. Couillard, P. S. Whitfield, I. J. Davidson, *Chem. Mater.*, 2011, **23**, 5446.
15 C. Deng, S. Zhang, S.Y. Yang, *J. Alloy Compd.*, 2009, **487**, L18.
16 I. Belharouak, A. Abouimrane, K. Amine, *J. Phys. Chem. C*, 2009, **113**, 20733.
17 K. Gao, C.S. Dai, J. Lv, S.D. Li, *J. Power Source*, 2012, **211**, 97.
18 A. Kokalj, R. Dominko, G. Mali, A. Meden, M. Gaberscek, J. Lamnik, *Chem. Mater.*, 2007, **19**, 3633.
19 C. Delacourt, L. Laffont, R. Bouchet, C. Wurm, J.-B. Leriche, M. Morcrette, J.-M. Tarascon, C. Masquelier, *J. Electrochem. Soc.*, 2005, **152**, A913.
20 T. Muraliganth, K. R. Stroukoff, A. Manthiram, *Chem. Mater.*, 2010, **22**, 5754.
21 M. Kuezma, S. Devaraj, P. Balaya, *J. Mater. Chem.*, 2012, **22**, 21279.
22 D. Rangappa, K. D. Murukanahally, T. Tomai, A. Unemoto, I. Honma, *Nano lett.*, 2012, **12**, 1146.
23 D.M. Kempaiah, D. Rangappa, I. Honma, *Chem. Commun.*, 2012, **48**, 2698.

Electronic Supplementary Material (ESI) for Chemical Communications

Supplementary Data

Experimental

***Synthesis*:** The organic-inorganic hybrid polymers with the composition of 40 wt% SiO_2 (COMPOCERAN P501) and 70wt% SiO_2 (COMPOCERAN HBP70) in their hardening resins were kindly supplied by Arakawa Chemical Industries Ltd. An aqueous solution of $LiOH{\cdot}H_2O$ was dropwise added under magnetic stirring to a mixed ethanol solution containing the hybrid polymer and $Mn(CH_3COO)_2{\cdot}4H_2O$ with the stoichiometric molar ratio (Li/Mn/Si=2/1/1). The solution was stirred for 12 h at room temperature and then dried at 100 °C to evaporate ethanol and water. The residue was ball-milled at 300 rpm for 2 h and then was pre-calcined at 500 °C for 2 h in an Ar atmosphere, followed by the ball-milling for 36 h in ethanol and the calcination at 650 °C for 20 h. A nanocomposite of Li_2MnSiO_4 and carbon nanotubes (CNTs) was also synthesized by the similar manner. Single-walled CNTs (ASP-100F, Hanwha Nanotech Corp.) were dispersed in an ethanol by an ultrasound sonication (40 W, 42 kHz) for 1 h, and then COMPOCERAN HBP70, $Mn(CH_3COO)_2{\cdot}4H_2O$ and an aqueous LiOH were added to this solution in order under the sonication for 1 h to form a gel. The mixing ratio of CNTs/HBP70 was 1/14 by weight. The obtained gel was subjected to dryness, ball-milling and calcination treatments at the same conditions as mentioned above. The samples obtained by using COMPOCERAN P501 and HBP70 are abbreviated as LMS-P501 and LMS-HBP70, respectively. The LMS-HBP70 including CNTs is denoted as LMS-HBP70-CNT. A Li_2MnSiO_4 sample without CNTs, denoted as Bulk-LMS, was synthesized as a reference by using $Si(CH_3COO)_4$ instead of the hybrid polymer at the same synthetic conditions except for the final calcination condition of 700 °C for 24 h to yield a single crystalline phase.

***Instrumental Analysis*:** X-ray diffraction (XRD) patterns of samples were obtained on a Rigaku RINT-2200 diffractometer using Cu Kα radiation. The morphology of samples was investigated by scanning electron microscopy (SEM, JEOL JCM-5100), transmission electron microscopy (TEM, JEOL JEM-2010UHR) and N_2 adsorption/desorption isotherms (BEL Japan BELSORP-mini). The composition of Li, Mn and Si in samples was analyzed by induced coupled plasma atomic emission spectroscopy (Horiba, ULTIMA2). The amount of carbon remained in the samples was determined by elemental analysis (Parkin-Elmer 2400II analyzer). Raman spectra of samples were taken by using JASCO RMP-210 with 532 nm laser (100 mW). Electrochemical charge-discharge curves were measured on an electrochemical analyzer (Hokuto Denko, HJ1001SD8) using a beaker-type three-electrode cell with metallic Li as a counter and reference electrode at room temperature. The electrolyte used was a 1.0 mol dm^{-3} solution of $LiPF_6$ in ethylene carbonate/dimethyl carbonate (1/1 by volume). The composite samples mixed with poly(tetrafluoroethylene) (PTFE) and additionally acetylene black (AB) were pressed on Al mesh, and then were used as working electrodes; the weight ratio of sample/AB/PTFE was 62.5/25/12.5 for Bulk-LMS, 85/10/5 for LMS-HBP70, and 90/0/10 for LMS-P501 and LMS-HBP70-CNT. To minimize the effect of IR drop associated with the electrolyte resistance, the tip of a capillary in connection to the reference electrode was placed as close as possible to the working electrode. The electrode was charged by a constant current–constant voltage (CC–CV) mode and subsequent discharged by the CC mode. The CC mode measurement was carried out at the current density of 16.6 mA g^{-1} (C/20, 1C = 333 mA g^{-1}) based on LMS weight. The cut-off current of CV mode was set at 1.66 mA g^{-1}. The discharge process was carried out by the CC mode to the cut-off potential of 1.5 V vs. Li^+/Li. The charge-discharge property of CNTs was also measured by the same manner using a working electrode of a mixture of CNTs and PTFE (CNTs/PTFE = 90/10 by weight) pressed onto Al mesh.

Table S1 Atomic ratio of Li, Si and Mn in the samples

Sample	Li	Mn	Si
Bulk-LMS	2.10	1.00	1.33
LMS-P501	2.08	1.00	1.22
LMS-HBP70	1.92	1.00	1.29
LMS-HBP70-CNT	2.08	1.00	1.37

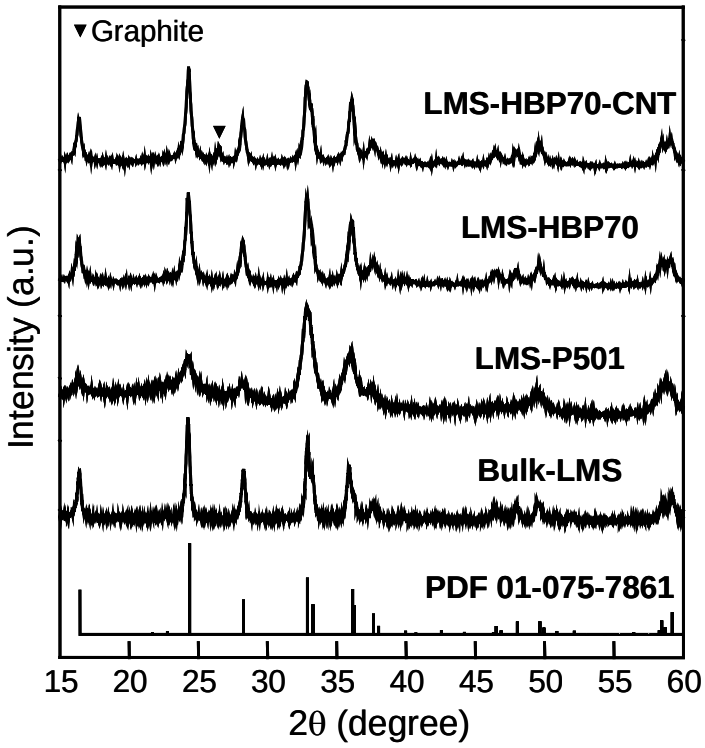

Fig. S1 XRD patterns of the samples.

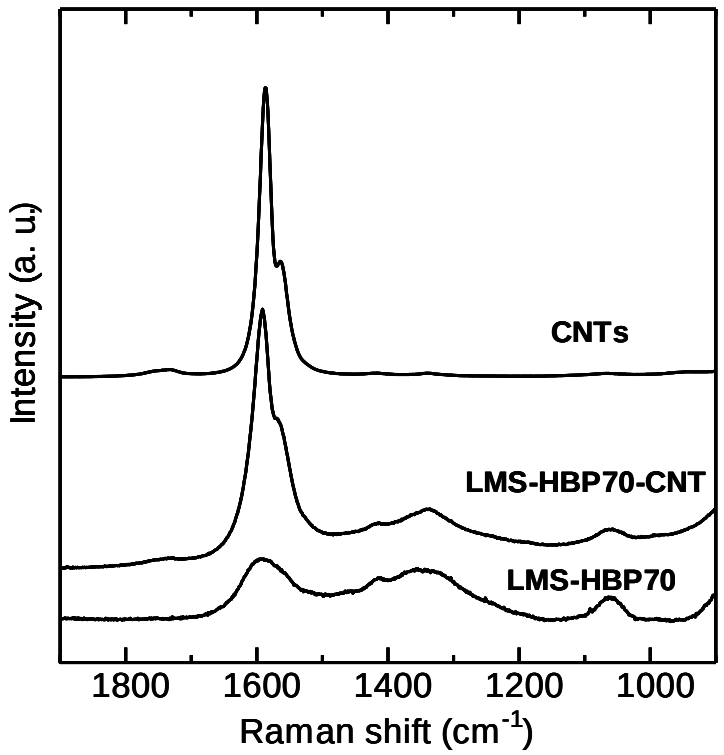

Fig. S2 Raman spectra of CNTs, LMS-HBP70-CNT and LMS-HBP70.

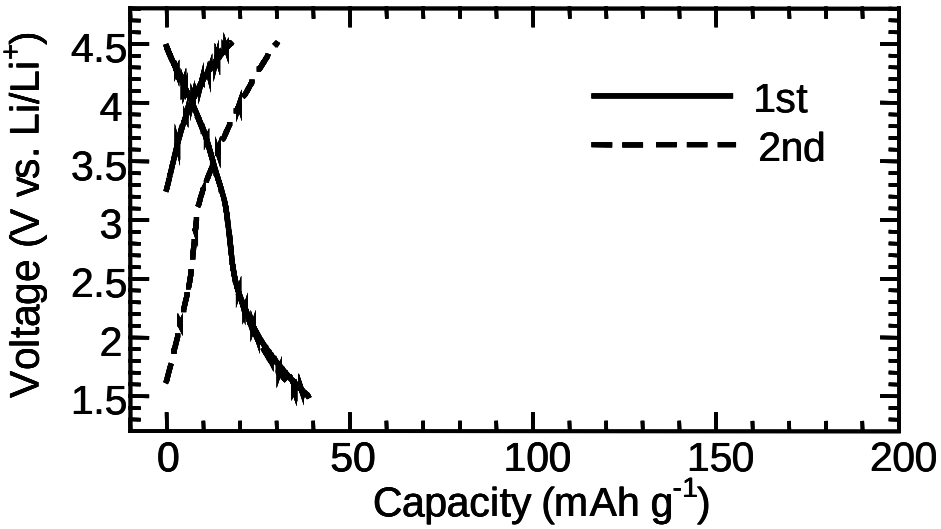

Fig. S3 1st and 2nd charge-discharge curves of CNTs.